BPTF activates the MAPK pathway through coexpression with Raf1 to promote proliferation of T-cell lymphoma

DONGYU BAI[1*], YONG ZHOU[2*], FAYAN SHEN[1], DEHONG GAO[1], WENHAO SUO[1], HAIPING ZHANG[1] and HENG LI[3]

[1]Department of Pathology; [2]Department of Hematology, The First Affiliated Hospital of Xiamen University, Xiamen, Fujian 361003; [3]Department of Pathology, The First Affiliated Hospital of Harbin Medical University, Harbin, Heilongjiang 150000, P.R. China

Received August 19, 2020; Accepted March 4, 2021

DOI: 10.3892/ol.2022.13344

Abstract. The aim of the present study was to explore the role and biological function of bromodomain PHD finger transcription factor (BPTF) in T-cell lymphoma. Reverse transcription-quantitative PCR (RT-qPCR), western blotting, immunohistochemistry and bioinformatics analysis were used to determine the expression levels of BPTF and Raf1 in T-cell lymphoma tissues and matched adjacent normal tissues. RT-qPCR and western blot analyses were used to examine the role of BPTF in the activation of MAPK signaling. The function of BPTF and Raf1 in T-cell lymphoma was investigated through *in vitro* and *in vivo* assays (MTT assay, colony formation assay, flow cytometry, western blotting, tumor xenograft model and TUNEL assay) following silencing and overexpression experiments in Hut-102 cells. The results demonstrated that BPTF and Raf1 were overexpressed in T-cell lymphoma tissues compared with normal tissues, and high expression of BPTF or Raf1 was associated with advanced clinical stage. BPTF promoted the activation of the MAPK pathway and was coexpressed with Raf1 in T-cell lymphoma tissues. Functional assays demonstrated that silencing of BPTF or Raf1 in Hut-102 cells suppressed cell proliferation and induced apoptosis. Furthermore, the carcinogenic effect of BPTF was confirmed by xenograft experiments in nude mice. The present findings suggested that BPTF may function as a crucial oncogenic factor and may serve as a novel therapeutic target in T-cell lymphoma.

Correspondence to: Professor Haiping Zhang, Department of Pathology, The First Affiliated Hospital of Xiamen University, 55 Zhenhai Road, Xiamen, Fujian 361003, P.R. China
E-mail: zhping3398@163.com

Professor Heng Li, Department of Pathology, The First Affiliated Hospital of Harbin Medical University, 23 Post Office Street, Harbin, Heilongjiang 150000, P.R. China
E-mail: heng_6306@163.com

*Contributed equally

Key words: bromodomain PHD finger transcription factor, Raf1, MAPK pathway, T-cell lymphoma

Introduction

T-cell lymphoma accounts for 10-15% of non-Hodgkin's lymphomas (1). In 2008, the World Health Organization classified T-cell lymphoma into different pathological subtypes: T-cell and natural killer (NK) cell lymphoma/leukemia, which originate from lymph nodes, extranodal tissues or skin (2,3). The prognosis of mature or peripheral T-cell lymphoma is worse compared with that of aggressive B-cell lymphoma (4,5). Therefore, the key to improving the prognosis of T-cell lymphoma is to determine the biological characteristics of T-cell lymphoma cells.

As a core subunit of the nucleosome-remodeling factor (NURF) complex, bromodomain PHD finger transcription factor (BPTF) serves crucial roles in chromatin remodeling (6). BPTF is critical for epigenetic regulation of DNA accessibility and gene expression (7). Recently, its function in tumor progression has attracted increased attention (8). BPTF has recently been found to influence the course of cancer, particularly by directly activating oncogenic signaling or through synergistic interactions with other key protein factors (9,10). To date, there is no relevant research report of BPTF in T-cell lymphoma, and thus the present study aimed to explore its regulatory mechanism and biological function in T-cell lymphoma.

Abnormal activation of the MAPK signaling pathway has an important role in cell malignant transformation and evolution (11). Multiple reports have demonstrated that MAPKs are significantly associated with the occurrence and development of breast cancer, ovarian cancer, esophageal cancer, colon cancer, gastric cancer, liver cancer and other tumors (12,13). The present study demonstrated that BPTF was highly expressed in cell lines and tissues of T-cell lymphoma. In addition, it was observed that BPTF and Raf1 were coexpressed in T-cell lymphoma cells. Silencing BPTF inhibited the activation of the MAPK pathway. Raf1 was also demonstrated to be highly expressed in cell lines and tissues of T-cell lymphoma. Silencing BPTF or Raf1 induced apoptosis in T-cell lymphoma cells. In summary, the current results suggested that BPTF promoted the proliferation of T-cell lymphoma by activating

the MAPK pathway. BPTF may serve as a molecular target for the treatment of T-cell lymphoma.

Materials and methods

Patients and tissue specimens. In the present study, 30 human cancerous lymph node tissues and matched adjacent nontumor tissues were obtained from patients who underwent lymph node resection between November 2016 and December 2019 in the Department of Pathology, the First Affiliated Hospital of Xiamen University (Xiamen, China). The overall experimental scheme was approved by the Ethics Committee of the First Affiliated Hospital of Xiamen University (approval no. KY-2018-014). All patients had signed informed consent. The clinical features of the patients, including age, sex, lymph node metastasis status, lactate dehydrogenase (LDH) levels and clinical stage, were collected from their medical records and listed in Table I.

Cell lines and culture. The human T cell line (H9) and human T-cell lymphoma cell line (Hut-102) were purchased from the Cell Resource Center, Shanghai Institute of Life Sciences, Chinese Academy of Sciences (Shanghai, China). They were cultured in 1640 medium (cat. no. 22400121; Thermo Fisher Scientific, Inc.) containing 10% fetal bovine serum (cat. no. 10099141C; Thermo Fisher Scientific, Inc.) and penicillin-streptomycin (cat. no. C0222; Beyotime Institute of Biotechnology) at 37˚C and 5% CO_2.

Mission short hairpin (sh) RNA series (cat. no. CSTVRS; Sigma-Aldrich; Merck KGaA) vectors were used for RNA silencing. shRNA probes TRCN0000016819 and TRCN0000001066 were used to silence BPTF and Raf1, respectively. A nontargeting shRNA (cat. no. SHC312V; Sigma-Aldrich; Merck KGaA) was used as the negative control (NC). PCMV3 (cat. no. NM_005228.3; SinoBiological, Inc.) was used as the overexpression vector to construct PCMV3-BPTF recombinant plasmid; blank vector was used as the control. The constructs were transfected into Hut-102 cells using Lipofectamine 3000 transfection reagent (cat. no. L3000001; Thermo Fisher Scientific, Inc.). Hut-102 cell lines stably transfected with NC, shBPTF or shRaf1 were constructed.

Tumor xenograft model. Four-week-old female BALB/cA nude mice (n=30) were purchased from the Shanghai Experimental Animal Center, Chinese Academy of Sciences. The study protocol was approved by the Experimental Animal Ethics Committee of the First Affiliated Hospital of Xiamen University (Xiamen, China; approval no. 2019-231). During the experiment, animal handling and care were carried out according to the National Institutes of Health Guide for the Care and Use of Laboratory Animals (NIH Publications no. 8023, revised 1978). Hut-102 cells stably transfected with nontargeting shRNA or shBPTF were inoculated on the backs of nude mice ($3x10^6$ cells per mouse) after light anesthesia using 37.5 mg/kg pelltobarbitalum natricum. The total experimental period was three weeks. The behavior and health of the nude mice were observed every day and the experiment was terminated in time for abnormal individuals. The maximum diameter of the tumor was 0.71 cm. The tumors were removed using resection, photographed using a camera (model E-PL9; Olympus Corporation) and weighed after all the mice were sacrificed using intraperitoneal injection of 200 mg/kg pelltobarbitalum natricum. Before euthanasia, carprofen (cat. no. V1074; InvivoChem Co., Ltd.; 5 mg/kg) was injected subcutaneously to relieve the pain of mice (14,15). The tumor volume was calculated using the following formula: $V = (\text{length} \times \text{width}^2)/2$.

MTT assay. Adherent cells (Hut-102 cell lines stably expressing NC, shBPTF or shRaf1) were cultured in 96-well plates for 24 h at a density of 5,000 cells per well. The original medium was discarded, and 100 μl serum-free DMEM and 10 μl (5 mg/ml) MTT (cat. no. 88417; Sigma-Aldrich; Merck KGaA) were added to each well. After 4 h, the reaction medium was discarded, and the formazan crystals were fully dissolved in 100 μl DMSO. The absorbance was measured at 570 nm using a microplate reader (Multiskan FC; Thermo Fisher Scientific, Inc.). Each experiment was repeated three times.

Clone formation assay. Adherent cells (Hut-102 cell lines stably expressing NC, shBPTF or shRaf1) were cultured in 6-well plates for ~2 weeks at a density of 200 cells per well. When the clone number of a single group reached >70, the culture medium was discarded, and the cells were fixed using methanol for 30 min. The fixed cells were stained with 0.5% crystal violet and photographed using a camera (model E-PL9; Olympus Corporation).

Annexin V/propidium iodide (PI) assay. Cells were digested with trypsin-EDTA solution (cat. no. T4049; Sigma-Aldrich; Merck KGaA), which was removed by centrifugation at 168 x g at room temperature for 10 min. Then, the cells were washed three times with sterile PBS and resuspended in 500 μl Annexin V/PI binding solution (cat. no. APOAF-20TST; Sigma-Aldrich; Merck KGaA). The cell suspension was stained with 10 μl PI and 5 μl Annexin V-FITC (cat. no. APOAF-20TST; Sigma-Aldrich; Merck KGaA at room temperature for 30 min. The cells were detected by flow cytometry (model NOVOCyte 2060R; ACEA Biosciences, Inc.) using the F1 channel (Annexin V-FITC) and F2 channel (PI). NovoExpress software v.1.2.4.1602 (ACEA Biosciences, Inc.) was used to analyze the results of flow cytometry.

Cell cycle distribution assays. Cells were digested with trypsin-EDTA solution (cat. no. T4049; Sigma-Aldrich; Merck KGaA), which was removed by centrifugation at 161 x g at room temperature for 10 min. Then, the cells were washed three times with sterile PBS and fixed by adding 70% ethanol at -20˚C overnight. The cell suspension was washed twice with PBS and stained with 400 μl PI (cat. no. P4864; Sigma-Aldrich; Merck KGaA) in the dark at 4˚C for 30 min. Cell cycle distribution was detected by flow cytometry using the F2 channel. NovoExpress software v.1.2.4.1602 (ACEA Biosciences, Inc.) was used to analyze the results of flow cytometry.

Western blot analysis. Total protein from H9 cells, Hut-102 cells (shNC, shBPTF, shRaf1, blank vector or overexpressed BPTF) or tissues (normal, T-cell lymphoma or xenograft tumors) was extracted by RIPA lysis buffer (cat. no. R0010; Beijing Solarbio

Table I. Clinicopathological features of 30 patients with T-cell lymphoma.

Clinicopathological feature	Samples (n=30)	P-value
Age (years)		
≤60	21	0.014
>60	9	
Sex		
Female	12	0.278
Male	18	
Nodes		
Intranodal	23	0.021
Extranodal	7	
Serum LDH levels		
Normal	6	0.035
Above normal	24	
Clinical stages		
I-II	23	0.041
III-IV	7	

LDH, lactate dehydrogenase.

Science & Technology Co., Ltd.) on ice for 30 min. Bicinchoninic acid (BCA) method was used to detect the protein concentration. Proteins (15 μg) of different sizes were separated by SDS-PAGE (10% separating gel and 5% concentrating gel). The protein in the PAGE gel was transferred to a polyvinylidene difluoride (PVDF) membrane and blocked in 5% skim milk at room temperature for 3 h. The PVDF membrane was incubated with the corresponding primary antibodies at room temperature for 2 h. After rinsing with Tris-buffered saline containing 0.05% Tween-20 (TBST) three times (10 min each), the PVDF membrane was incubated with secondary antibodies at room temperature for 1 h. The ECL Plus western blotting substrate (cat. no. 32132; Thermo Fisher Scientific, Inc.) was added to the PVDF membrane and detected by a multifunctional gel imaging system (model Gel Doc XR+; Bio-Rad Laboratories, Inc.). The relative amount of protein was quantitatively analyzed by densitometry using SageDetect software v.2.1.8.160722 (Beijing Sage Creation Science Co., Ltd.). Antibodies against the following proteins were used: BPTF (cat. no. ab72036; 1:2,000; Abcam), Raf1 (cat. no. ab137435; 1:1,000; Abcam), phosphorylated (p-) Raf1 S569 (cat. no. ab173539; 1:1,000; Abcam), MEK1 (cat. no. ab32091; 1:1,000; Abcam), p-MEK1-S298 (cat. no. ab96379; 1:1,000; Abcam), Erk1/2 (cat. no. WL01864; 1:500; Wanleibio Co., Ltd.), p-Erk1/2-Thr202/Tyr204 (cat. no. WLP1512; 1:500; Wanleibio Co., Ltd.), and β-actin (cat. no. WL01372; 1:3,000; Wanleibio Co., Ltd.). The secondary antibody was HRP-conjugated goat anti-rabbit immunoglobulin G (1:5,000; cat. no. A-11006; Thermo Fisher Scientific, Inc.).

RNA isolation and reverse transcription-quantitative PCR (RT-qPCR). Total RNA was isolated from the cells and tissues using a MicroElute Total RNA kit (cat. no. R6831-01; Omega Bio-Tek, Inc.). The RNA was reverse transcribed into cDNA using the PrimeScript RT reagent kit (cat. no. RR037A; Takara Biotechnology Co., Ltd.). The reverse transcription reaction conditions were 37˚C for 15 min and 85˚C for 5 sec. Reverse Transcription of RNA was performed using the PrimeScript RT reagent kit (cat. no. RR037A; TAKARA Inc.) on PCR instrument (model TC-E-48D; Hangzhou Bioer Technology Co. Ltd.). RT-qCR was performed using the SYBR Green qPCR Mix (cat. no. D7260; Beyotime Institute of Biotechnology) on an Applied Biosystems 7500 Real-Time PCR system (Thermo Fisher Scientific, Inc.). The qPCR reaction conditions were: 1 cycle of 95˚C for 10 sec, followed by 40 cycles of 94˚C for 5 sec and 60˚C for 34 sec, and finally 1 cycle of 95˚C for 15 sec, 60˚C for 1 min and 95˚C for 15 sec. The following primer sequences were used for qPCR: BPTF, forward, 5'-CCCAGGTGGTGATGAAGCAT-3' and reverse, 5'-CCCAGGTGGTGATGAAGCAT-3'; Raf1, forward, 5'-CGCTTAGATTGGAATACTGA-3' and reverse, 5'-AAAGGTGAAGGCGTGAG-3'; and GAPDH, forward, 5'-ATGACATCAAGAAGGTGGTGAAGCAGG-3' and reverse, 5'-GCGTCAAAGGTGGAGGAGTGGGT-3'. GAPDH was used as an internal reference gene. Relative fold changes in mRNA expression were calculated using the formula $2^{-\Delta\Delta Cq}$ (16).

Immunohistochemistry. The transplanted tumor tissues in nude mice and clinical tumor samples were fixed with 4% paraformaldehyde at room temperature for 24 h. The samples were embedded in paraffin, and sectioned (5-μm thickness). After dewaxing and hydration, the samples were incubated with 3% hydrogen peroxide at room temperature for 10 min. The samples were treated with 0.01 mol/l sodium citrate buffer solution (pH 6.0) at 95˚C for 10 min for antigen retrieval. The samples were incubated in goat serum (cat. no. C0265; Beyotime Institute of Biotechnology) at room temperature for 20 min. Then, the samples were incubated with the corresponding primary antibodies at 4˚C overnight. After rinsing with PBS three times (5 min each), the samples were incubated with secondary antibodies at 37˚C for 1 h. The samples were colored according to the instructions of the 3,3' diaminobenzidine color developing kit (cat. no. P0202; Institute of Biotechnology) and visualized using a light microscope (model CX41; Olympus Corporation).

TUNEL assay. The transplanted tumor tissues in nude mice were fixed using 4% paraformaldehyde for 24 h at room temperature. The fixed tumor tissues were embedded in paraffin and sectioned to 5-μm thickness. Paraffin tissue was dewaxed with xylene and gradient ethanol. The samples were treated with 20 μg/ml protease K without DNase at 37˚C for 30 min. The samples were washed twice with PBS for 10 min each time. TUNEL solution (50 μl) was added to the sample and incubated at 37˚C for 60 min. The samples were washed twice with PBS for 10 min each time. DAPI (5 μg/ml) (cat. no. C1002; Beyotime Institute of Biotechnology) was used for nuclear staining at room temperature for 10 min. The samples were washed twice with PBS for 10 min each time. After drying, the slides were sealed with a sealing solution containing an anti-fluorescence quenching agent. The samples were observed under a fluorescence microscope (model CKX53; Olympus Corporation) in 10 fields of view with a x200 magnification.

Statistical analysis. All experimental data were analyzed by SPSS 21.0 software (IBM Corp.) and expressed as the

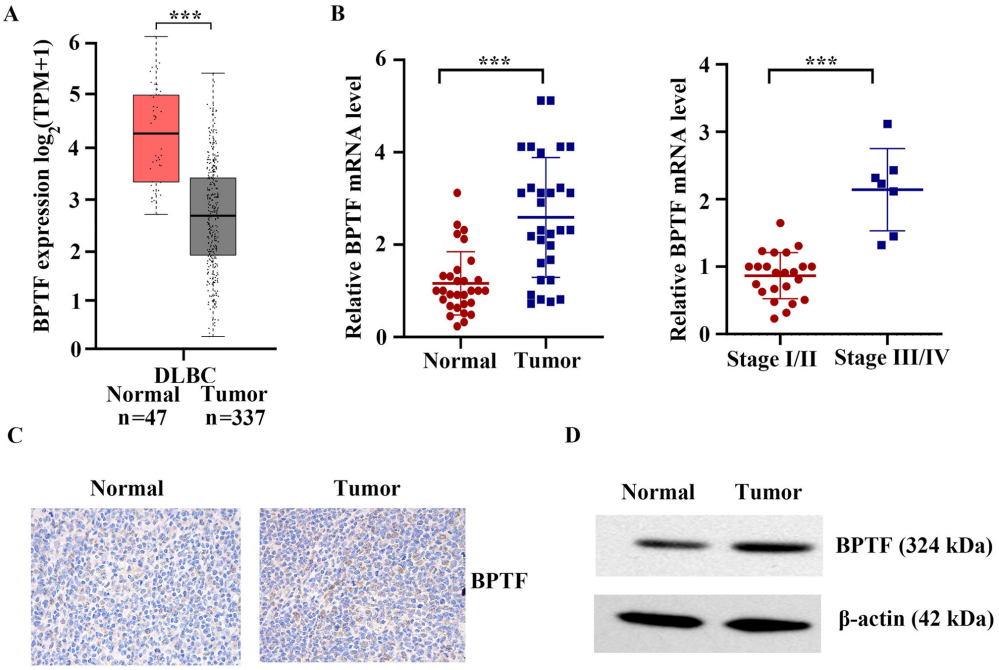

Figure 1. BPTF is overexpressed in T-cell lymphoma tissues. (A) BPTF expression in lymphoid neoplasm DLBC and normal tissues was analyzed from mRNA sequencing data from TCGA database. Red denotes cancer tissue, and gray denotes normal tissue. (B) mRNA expression levels of BPTF in cancerous lymph nodes vs. adjacent normal tissues from T-cell lymphoma patients, and in stage III/IV vs. stage I/II tumor tissues. (C) Immunohistochemistry staining of BPTF in cancerous lymph nodes or adjacent normal tissues from T-cell lymphoma patients. Magnification, x400. (D) Western blot analysis of protein expression of BPTF in lymph nodes or adjacent normal tissues from T-cell lymphoma patients. ***P<0.001. BPTF, bromodomain PHD finger transcription factor; DLBC, diffuse large B-cell lymphoma; TCGA, The Cancer Genome Atlas.

means ± standard deviation (SD). Experiments were repeated at least three times. Unpaired Student's t-test was used for statistical analysis between two independent samples, while paired Student's t-test was used for statistical analysis between two paired samples. Bonferroni's correction was used for one-way ANOVA among multiple groups. Chi-square test was used to analyze the distribution of clinical variables (age, sex, nodes, serum LDH levels, clinical stages). P<0.05 was considered to indicate a statistically significant difference.

Results

BPTF is upregulated in clinical T-cell lymphoma tissues. The Cancer Genome Atlas (TCGA) database (https://portal.gdc.cancer.gov/) was used to analyze the mRNA differences between lymphoma tissues and adjacent normal tissues. As shown in Fig. 1A, the mRNA expression levels of BPTF in lymphoid neoplasm diffuse large B-cell lymphoma (DLBC) were significantly higher compared with those in normal tissues (P<0.001). The present study further detected the mRNA expression levels of BPTF in 30 human cancerous lymph node tissues and matched adjacent nontumor tissues from patients who were diagnosed with T-cell lymphoma. The results demonstrated that the mRNA expression levels of BPTF in cancerous lymph node tissue were significantly higher compared with those in normal tissues (P<0.001; Fig. 1B). Compared with stage I/II, BPTF mRNA was significantly higher expressed in stages III/IV T-cell lymphoma (P<0.001; Fig. 1B). The results of immunohistochemistry and western blot analyses also indicated that the protein expression of BPTF in cancerous lymph node tissue was significantly higher compared with that in normal tissues (Fig. 1C and D). Altogether, the present results indicated that BPTF upregulation may have a critical role in the development and progression of T-cell lymphoma.

Activation of the MAPK pathway by coexpression of BPTF and Raf1. Western blot analysis results demonstrated that the expression and phosphorylation levels of MAPK pathway-related proteins in T-cell lymphoma tissues were significantly higher compared with those in normal tissues (Fig. 2A). To further explore the function of BPTF in T-cell lymphoma, shRNA silencing and overexpression experiments were performed. As shown in Fig. 2B and C, RT-qPCR results demonstrated that the expression of BPTF in Hut-102 cells transfected with shBPTF was 34.67±6.66% of that in the control group (transfected with NC shRNA) and the expression of BPTF in Hut-102 cells overexpressing BPTF was 4.35±1.04-fold of that in the control group (transfected with blank vector). The results of western blot analysis and RT-qPCR were consistent (Fig. 2C and C). Western blot results showed that MAPK pathway-related proteins and their phosphorylation levels were downregulated in BPTF-silenced Hut-102 cells (Fig. 2D). The potential interaction between BPTF and MAPK pathway-related proteins was analyzed using the STRING website (https://string-db.org/cgi/input?sessionId=b55z0svNSjXZ&input_page_active_form=multiple_identifiers) (17). The results showed that BPTF interacted with MYC and Raf1 (Fig. 2E). Notably, BPTF and Raf1 were coexpressed. The correlation analysis of BPTF and Raf1 from TCGA database showed that there was a positive correlation between them (R=0.78, P<0.001;

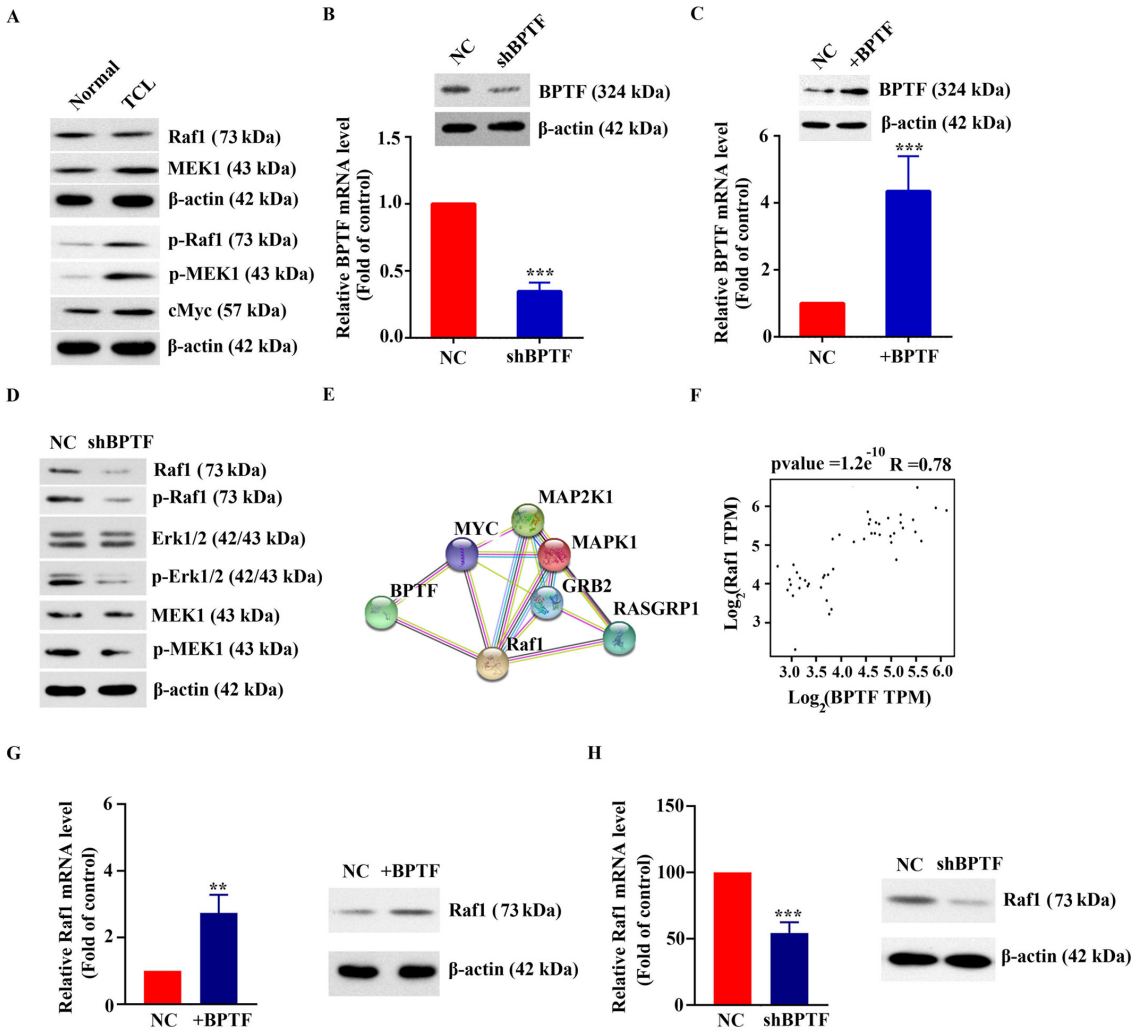

Figure 2. Activation of the MAPK pathway by coexpression of BPTF and Raf1. (A) Western blot analysis of MAPK pathway-related proteins in cancerous lymph nodes or adjacent normal tissues from TCL patients. (B) mRNA and protein expression levels of BPTF in Hut-102 cells following transfection with NC or shBPTF. (C) mRNA and protein expression levels of BPTF in Hut-102 cells transfected with NC (empty vector) or with a BPTF-overexpressing vector. (D) Western blot analysis of MAPK pathway-related in Hut-102 cells transfected with NC or shBPTF. (E) The interaction between BPTF and MAPK pathway-related proteins was analyzed using the STRING website. (F) Correlation analysis of BPTF and Raf1 expressions from TCGA database. (G) mRNA and protein expression levels of Raf1 in Hut-102 cells overexpressing BPTF. (H) mRNA and protein expression levels of Raf1 in Hut-102 cells following BPTF silencing. **P<0.01 and ***P<0.001. BPTF, bromodomain PHD finger transcription factor; TCL, T-cell lymphoma; NC, negative control; sh, short hairpin; MAP2K1, mitogen-activated protein kinase kinase 1; MAPK1, mitogen-activated protein kinase 1; GRB2, growth factor receptor bound protein 2; RASGRP1, RAS guanyl releasing protein 1.

Fig. 2F). RT-qPCR results showed that mRNA expression levels of Raf1 were increased to 2.74±0.55-fold of the control (P<0.01) when Hut-102 cells overexpressed BPTF (Fig. 2G). In addition, the mRNA expression levels of Raf1 were 54.26±8.14% of the control (P<0.001) when BPTF was silenced in Hut-102 cells (Fig. 2H). Western blot results were consistent with RT-qPCR results (Fig. 2G and H). The present findings indicated that high expression of BPTF may activate the MAPK pathway, and that BPTF and Raf1 may be coexpressed in T-cell lymphoma.

Raf1 is upregulated in clinical T-cell lymphoma tissues. TCGA database was used to analyze the mRNA differences between lymphoma tissues and adjacent normal tissues. As shown in Fig. 3A, the mRNA expression levels of Raf1 in lymphoid neoplasm DLBC were significantly higher compared with those in normal tissues (P<0.001). The mRNA expression of Raf1 was further detected in the 30 human cancerous lymph node tissues and matched adjacent nontumor tissues, collected for the presents study. The results showed that the mRNA expression levels of Raf1 in cancerous lymph node tissue were significantly higher compared with those in normal tissues (P<0.001; Fig. 3B). Compared with stage I/II, Raf1 mRNA was more highly expressed in stages III/IV T-cell lymphatic carcinoma (P<0.001; Fig. 3B). The results of immunohistochemistry and western blot also indicated that the protein expression of Raf1 in cancerous lymph node tissue was markedly higher compared with that in normal tissues (Fig. 3C and D). Altogether, the present results indicated that Raf1 upregulation may have a critical role in the development and progression of T-cell lymphoma.

Effect of BPTF and Raf1 on the proliferation of T-cell lymphoma cells. The human T-cell line H9 and human T-cell

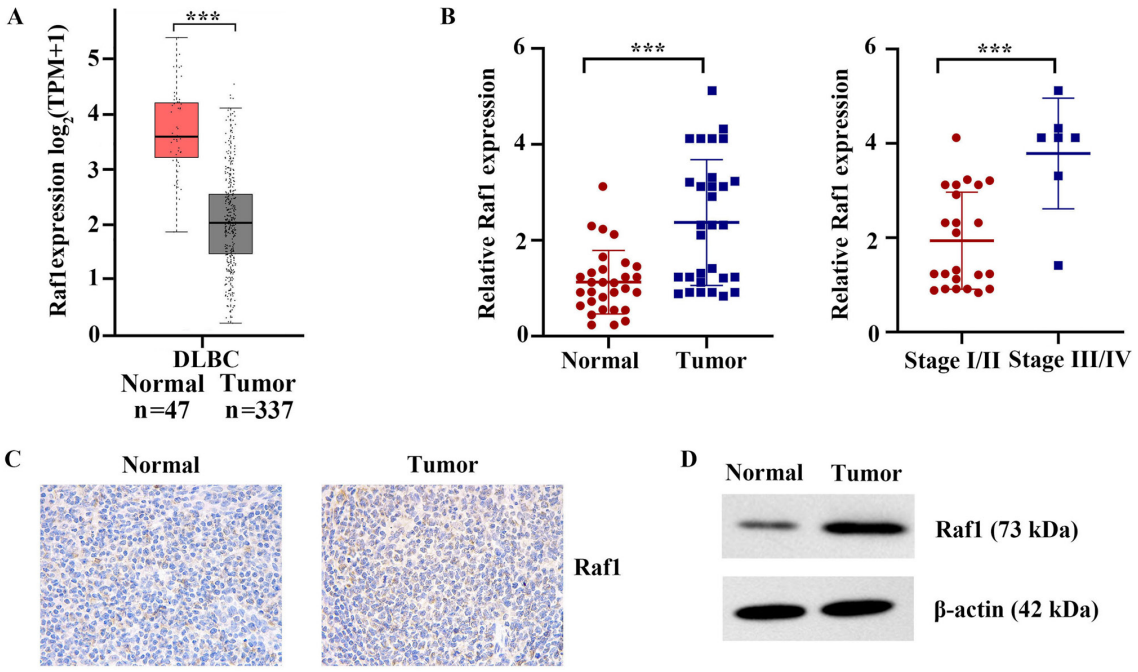

Figure 3. Raf1 is overexpressed in T-cell lymphoma tissues. (A) Raf1 expression in lymphoid neoplasm DLBC and normal tissues was analyzed from mRNA sequencing data from TCGA database. Red denotes cancer tissue, and gray denotes normal tissue. (B) mRNA expression levels of Raf1 in cancerous lymph nodes vs. adjacent normal tissues from T-cell lymphoma patients, and in stage III/IV vs. stage I/II tumor tissues. (C) Immunohistochemistry staining of Raf1 in cancerous lymph nodes or adjacent normal tissues from T-cell lymphoma patients. Magnification, x400. (D) Western blot analysis of protein expression of Raf1 in cancerous lymph nodes or adjacent normal tissues from T-cell lymphoma patients. ***P<0.001. DLBC, diffuse large B-cell lymphoma; TCGA, The Cancer Genome Atlas.

lymphoma cell line Hut-102 were used as cell models. As shown in Fig. 4A, the mRNA expression levels of BPTF and Raf1 in Hut-102 cells were 3.74±0.54 (P<0.001) and 4.11±0.55 (P<0.001) times higher compared with those in H9 cells, respectively. Western blot results were consistent with the RT-qPCR results (Fig. 4B). Fig. 4C demonstrates the successful silencing of Raf1 in Hut-102 cells by shRNA: RT-qPCR results showed that the mRNA expression of Raf1 in Hut-102 cells following Raf1 silencing was 32.11±5.57% of that in the control group (transfected with NC) and the results of western blot analysis were consistent with that of RT-qPCR. The results of the cell viability assay showed that the numbers of viable Hut-102 cells were significantly decreased following BPTF or Raf1 silencing (46.56±5.4 and 42.78±6% of the NC, respectively; P<0.001; Fig. 4D). The clone formation experiment showed that the number of clones in the Hut-102 cells transfected with the NC shRNA was higher than that of Hut-102 cells transfected with shBPTF or shRaf-1 (2.06±0.04-fold of the shBPTF, P<0.01; 1.78±0.11-fold of the shRaf1, P<0.05; Fig. 4E). Annexin V/PI staining experiments showed that the apoptosis rate of Hut-102 cells transfected with the NC shRNA (NC) was significantly lower than that of Hut-102 cells transfected with shBPTF or shRaf-1 (12.12±2.95% with shBPTF, P<0.001; 12.39±4.22% with shRaf1, P<0.001; Fig. 4F). Cell cycle phase distribution experiments showed that Hut-102 cells following BPTF or Raf-1 silencing remained in G1 phase compared with those in the NC group (Fig. 4G). Bax and Bcl-2 protein expression was detected by western blotting, and the gray value was used for relative quantification. The results revealed that the Bax/Bcl-2 signal ratio in Hut-102 cells following BPTF or Raf-1 silencing was significantly higher than that in Hut-102 cells transfected with the NC shRNA (6.01±0.3-fold of the NC, P<0.001; 4.29±0.23-fold of the NC, P<0.001; Fig. 4H). These results indicated that high expression of BPTF or Raf1 may promote the proliferation of T-cell lymphoma.

Effect of BPTF on tumor growth in vivo. Finally, a xenograft model was used to investigate the effect of BPTF on tumor growth *in vivo*. As shown in Fig. 5A, tumors in the shBPTF group grew smaller compared with those in the control group. RT-qPCR results confirmed that the expression of BPTF in the shBPTF cell-derived tumors was 28.22±2.65% of that in the control tumors and the result of western blot was consistent with that of RT-qPCR (Fig. 5B). The average volume of tumors in the shBPTF group was 26.65±10.63% that of the control group (P<0.001; Fig. 5C). The weight of tumors in the shBPTF group was 34.19±11.49% that of the control group (P<0.001; Fig. 5D). The results of the TUNEL assay showed that the tumors in the shBPTF group had a marked increase in apoptosis compared with the control group (Fig. 5E).

Discussion

Lymphomas mainly originate from lymph nodes and other lymphoid tissues. In recent years, the incidence rate of lymphoma has increased rapidly, ranking fifth in the world, which seriously threatens human health (18,19). There are many reports about the signaling pathways involved in the occurrence and development of lymphoma (20,21). Miller *et al* (22) reported that the MAPK signaling pathway influenced apoptosis in malignant lymphoid cells treated with glucocorticoids. Inhibition of MAPKs restored the drug sensitivity of a glucocorticoid-resistant clone in CEM-C1-15 cells. Sun *et al* (23) reported in a review that multiple signaling pathways (B cell

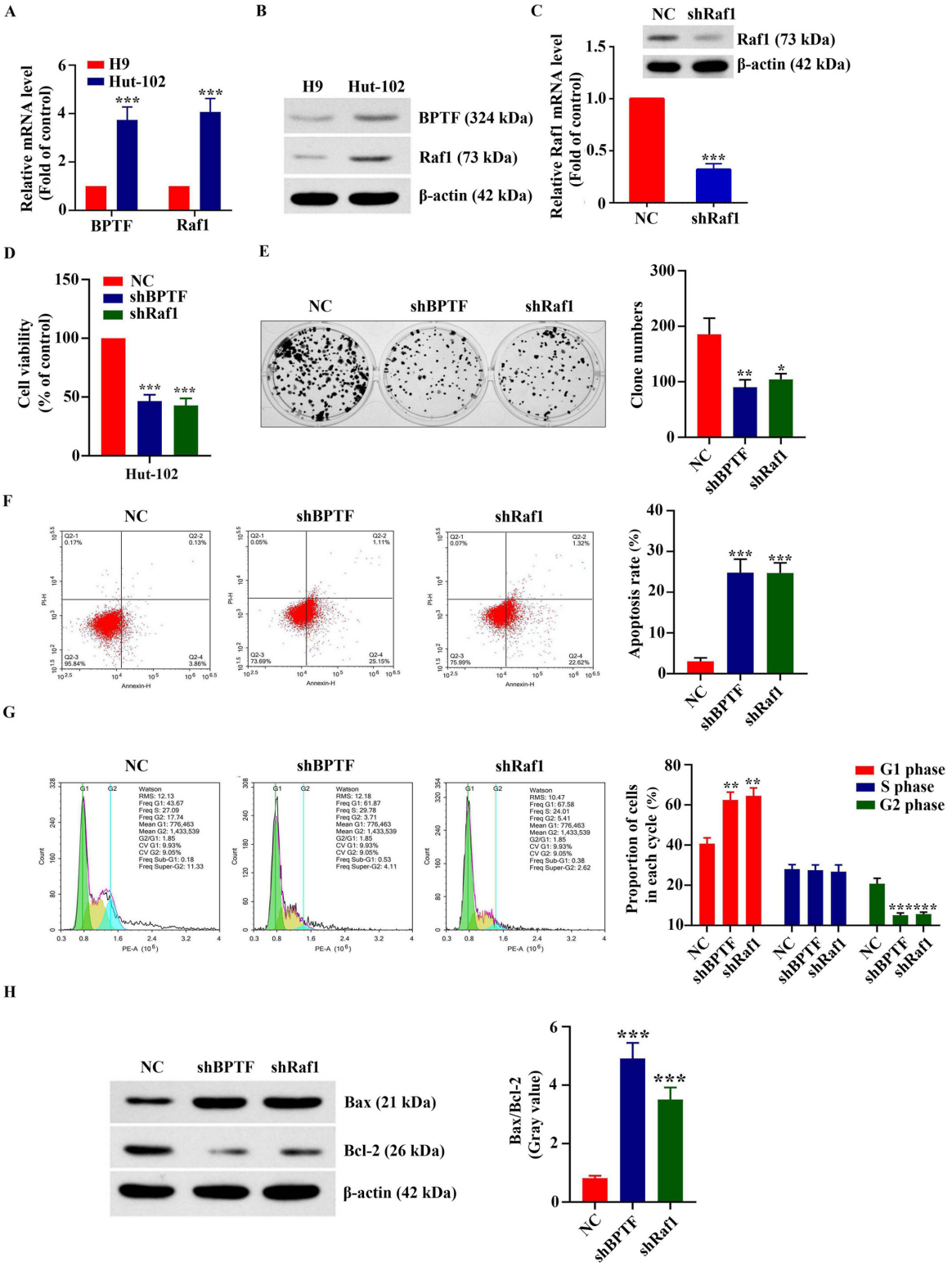

Figure 4. Effect of BPTF or Raf1 on the proliferation of T-cell lymphoma. (A) mRNA and (B) protein expression levels of BPTF and Raf1 in H9 cells and Hut-102 cells. ***P<0.001 vs. H9 cells. (C) Confirmation of successful silencing of Raf1 in Hut-102 cells by shRaf1. ***P<0.001 vs. NC. (D) Cell viability of Hut-102 cells transfected with shBPTF, shRaf1 or NC. MTT assays were performed 24 h after transfection. ***P<0.001 vs. NC. (E) Representative micrographs (left) and relative quantification (right) from colony formation assays. *P<0.05 and **P<0.01 vs. NC. (F) Flow cytometry plots and quantitative analysis of Annexin V/propidium iodide staining assay. ***P<0.001 vs. NC. (G) Flow cytometric analysis of cell cycle phase distribution assay. Histograms depict the proportion of Hut-102 cells in G1, S and G2 phases. **P<0.01 and ***P<0.001 vs. NC. (H) Western blot analysis of Bax, Bcl-2, and β-actin. The histogram depicts the signal ration of Bax/Bcl-2. ***P<0.001 vs. NC. BPTF, bromodomain PHD finger transcription factor; NC, negative control; sh, short hairpin.

receptor, NF-κB, PI3K/AKT/mTOR, and JAK/STAT signaling pathways) were involved in the development of lymphoma. This suggests that these molecular markers may be used as targets for diagnosis and treatment. The present study demonstrated that the MAPK pathway was abnormally activated in T-cell lymphoma tissues compared with normal tissues.

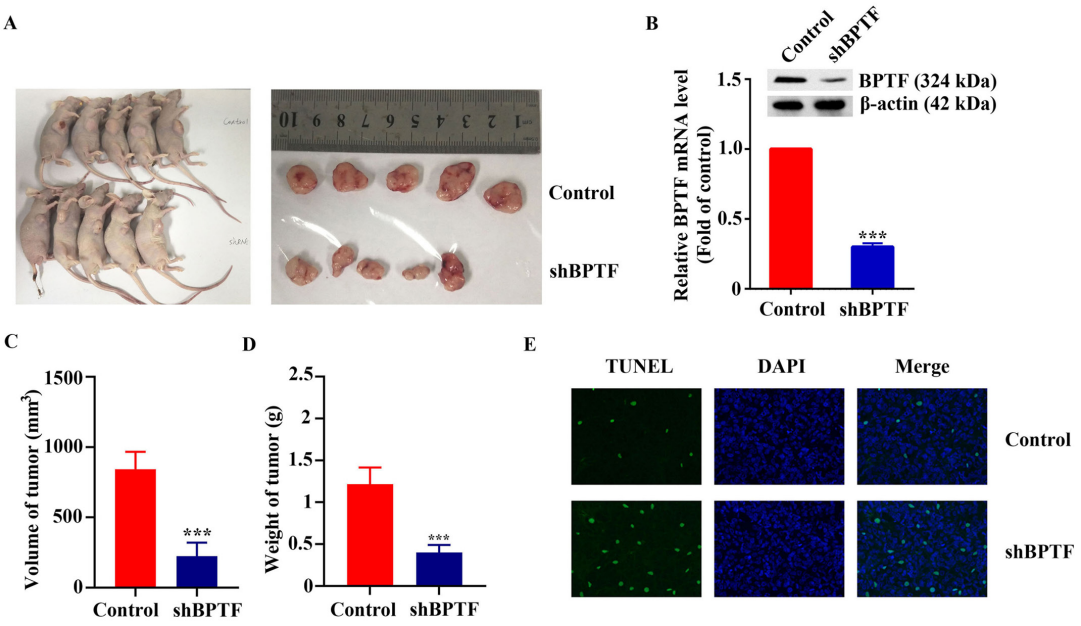

Figure 5. Effect of BPTF on tumor growth *in vivo*. (A) Photographs of nude mice and the resected xenograft tumors in the nontargeting shRNA (control) and shBPTF groups. (B) mRNA and protein expression levels of BPTF in the xenograft tumors of the control and the shBPTF groups. (C) Tumor volumes in the different groups. (D) Tumor weights in the different groups. (E) Representative images from TUNEL assay in the xenografts tumors from the two groups. Magnification, x100. ***P<0.001 vs. NC. BPTF, bromodomain PHD finger transcription factor; sh, short hairpin.

Furthermore, the present results revealed that the coexpression of BPTF and Raf1 was involved in the abnormal activation of the MAPK pathway in T-cell lymphoma.

As the core subunit of the NURF complex, BPTF has an important role in chromatin remodeling (24). In recent years, increasing attention has been given to its role in tumor development. Zhao *et al* (7) reported that BPTF promoted hepatocellular carcinoma (HCC) proliferation by targeting human telomerase reverse transcriptase and suggested that BPTF could be a potential molecular target for the treatment of HCC. Dai *et al* (8) reported that BPTF promoted lung cancer growth via cooperation with p50 NF-κB and regulation of cyclooxygenase-2 (COX-2) expression. That study suggested that the BPTF/p50/COX-2 axis could be a potential therapeutic target for lung cancer. The present study found that BPTF and Raf1 were abnormally overexpressed in T-cell lymphoma cells and tissues. The viability of human T-cell lymphoma cells (Hut-102) was decreased significantly after silencing BPTF or Raf1. Several cells showed early apoptosis accompanied by activation of the apoptosis factor Bax. Additionally, the cell cycle was blocked in G1 phase when BPTF or Raf1 were silenced in Hut-102 cells. Therefore, it can be speculated that the coexpression of BPTF and Raf1 is abnormally elevated, promoting the survival of T-cell lymphoma cells. The present study further confirmed the carcinogenic effect of BPTF in nude mice. Results from *in vivo* xenografting experiments revealed that tumors derived from BPTF-silenced cells grew more slowly than those derived from control cells. The tumors in the shBPTF group had a marked increase in apoptosis compared with the control group, as demonstrated by a TUNEL assay. Altogether, the present results indicated that BPTF and Raf1 upregulation may have a critical role in the development and progression of T-cell lymphoma. There is a coexpression relationship between BPTF and Raf1.

Oncogene signal transduction pathways and oncogene changes have an important role in the development of lymphoma. In the era of precision medicine, it is necessary and valuable to recognize the activation of these carcinogenic pathways and biomarkers (25,26). The present study identified abnormalities in the MAPK pathway in T cell lymphoma. It was further found that BPTF could activate the MAPK pathway by coexpression with Raf1 and promote the proliferation of T-cell lymphoma cells. These findings enrich the understanding of the pathogenesis of T-cell lymphoma and may provide a novel target and strategies for the treatment of T-cell lymphoma.

Acknowledgements

The authors would like to thank The Cancer Genome Atlas (TCGA) repository for providing data.

Funding

Support for this study was provided by the National Natural Science Foundation of China (grant no. 81800196).

Availability of data and materials

All data generated or analyzed during this study are included in this published article.

Authors' contributions

DB was responsible for the conception and writing of the overall research. YZ and FS were responsible for cell and animal experiments. DG and WS were responsible for the statistical analysis. HZ and HL were responsible for bioinformatics analysis, molecular biology experiments and data

proofreading. DB and HZ confirmed the authenticity of all the raw data. All authors read and approved the final manuscript.

Ethics approval and consent to participate

Experimental research involving patients was approved by the Ethics Committee of the First Affiliated Hospital of Xiamen University (Xiamen, China; approval no. KY-2018-014). All patients had signed informed consent. The animal protocol was approved by the Experimental Animal Ethics Committee of the First Affiliated Hospital of Xiamen University (Xiamen, China; approval no. 2019-231). The authors state that they have obtained appropriate institutional review board approval or have followed the principles outlined in the Declaration of Helsinki for all human or animal experimental investigations.

Patient consent for publication

Not applicable.

Competing interests

The authors declare that they have no competing interests.

References

1. Evens AM, Querfeld C and Rosen ST: T-cell non-Hogdkin's lymphoma. Cancer Treat Res 131: 161-220, 2006.
2. The world health organization classification of malignant lymphomas in Japan: Incidence of recently recognized entities. Lymphoma study group of Japanese pathologists. Pathol Int 50: 696-702, 2000.
3. Mugnaini EN and Ghosh N: Lymphoma. Prim Care 43: 661-675, 2016.
4. Nair R and Neelapu SS: The promise of CAR T-cell therapy in aggressive B-cell lymphoma. Best Pract Res Clin Haematol 31: 293-298, 2018.
5. Grimm KE and O'Malley DP: Aggressive B cell lymphomas in the 2017 revised WHO classification of tumors of hematopoietic and lymphoid tissues. Ann Diagn Pathol 38: 6-10, 2019.
6. Alkhatib SG and Landry JW: The nucleosome remodeling factor. FEBS Lett 585: 3197-3207, 2011.
7. Zhao X, Zheng F, Li Y, Hao J, Tang Z, Tian C, Yang Q, Zhu T, Diao C, Zhang C, *et al*: BPTF promotes hepatocellular carcinoma growth by modulating hTERT signaling and cancer stem cell traits. Redox Biol 20: 427-441, 2019.
8. Dai M, Hu S, Liu CF, Jiang L, Yu W, Li ZL, Guo W, Tang R, Dong CY, Wu TH and Deng WG: BPTF cooperates with p50 NF-κB to promote COX-2 expression and tumor cell growth in lung cancer. Am J Transl Res 11: 7398-7409, 2019.
9. Dar AA, Majid S, Bezrookove V, Phan B, Ursu S, Nosrati M, De Semir D, Sagebiel RW, Miller JR III, Debs R, *et al*: BPTF transduces MITF-driven prosurvival signals in melanoma cells. Proc Natl Acad Sci USA 113: 6254-6258, 2016.
10. Richart L, Real FX and Sanchez-Arevalo Lobo VJ: c-MYC partners with BPTF in human cancer. Mol Cell Oncol 3: e1152346, 2016.
11. Peluso I, Yarla NS, Ambra R, Pastore G and Perry G: MAPK signalling pathway in cancers: Olive products as cancer preventive and therapeutic agents. Semin Cancer Biol 56: 185-195, 2019.
12. Zou X and Blank M: Targeting p38 MAP kinase signaling in cancer through post-translational modifications. Cancer Lett 384: 19-26, 2017.
13. Rezatabar S, Karimian A, Rameshknia V, Parsian H, Majidinia M, Kopi TA, Bishayee A, Sadeghinia A, Yousefi M, Monirialamdari M and Yousefi B: RAS/MAPK signaling functions in oxidative stress, DNA damage response and cancer progression. J Cell Physiol: Feb 27, 2019 (Epub ahead of print).
14. Davis JA: Mouse and rat anesthesia and analgesia. Curr Protoc Neurosci: Jan 1, 2008 (Epub ahead of print).
15. Adams S and Pacharinsak C: Mouse anesthesia and analgesia. Curr Protoc Mouse Biol 5: 51-63, 2015.
16. Schmittgen TD and Livak KJ: Analyzing real-time PCR data by the comparative C(T) method. Nat Protoc 3: 1101-1108, 2008.
17. Szklarczyk D, Gable AL, Lyon D, Junge A, Wyder S, Huerta-Cepas J, Simonovic M, Doncheva NT, Morris JH, Bork P, *et al*: STRING v11: Protein-protein association networks with increased coverage, supporting functional discovery in genome-wide experimental datasets. Nucleic Acids Res 47: D607-D613, 2019.
18. Jiang M, Bennani NN and Feldman AL: Lymphoma classification update: T-cell lymphomas, Hodgkin lymphomas, and histiocytic/dendritic cell neoplasms. Expert Rev Hematol 10: 239-249, 2017.
19. Jaffe ES: Diagnosis and classification of lymphoma: Impact of technical advances. Semin Hematol 56: 30-36, 2019.
20. Yu L, Li L, Medeiros LJ and Young KH: NF-κB signaling pathway and its potential as a target for therapy in lymphoid neoplasms. Blood Rev 31: 77-92, 2017.
21. Yang W, Wang Y, Yu Z, Li Z, An G, Liu W, Lv R, Ma L, Yi S and Qiu L: SOX11 regulates the pro-apoptosis signal pathway and predicts a favorable prognosis of mantle cell lymphoma. Int J Hematol 106: 212-220, 2017.
22. Miller AL, Geng C, Golovko G, Sharma M, Schwartz JR, Yan J, Sowers L, Widger WR, Fofanov Y, Vedeckis WV and Thompson EB: Epigenetic alteration by DNA-demethylating treatment restores apoptotic response to glucocorticoids in dexamethasone-resistant human malignant lymphoid cells. Cancer Cell Int 14: 35, 2014.
23. Sun RF, Yu QQ and Young KH: Critically dysregulated signaling pathways and clinical utility of the pathway biomarkers in lymphoid malignancies. Chronic Dis Transl Med 4: 29-44, 2018.
24. Gong YC, Liu DC, Li XP and Dai SP: BPTF biomarker correlates with poor survival in human NSCLC. Eur Rev Med Pharmacol Sci 21: 102-107, 2017.
25. Nakagawa H and Fujita M: Whole genome sequencing analysis for cancer genomics and precision medicine. Cancer Sci 109: 513-522, 2018.
26. Pauli C, Hopkins BD, Prandi D, Shaw R, Fedrizzi T, Sboner A, Sailer V, Augello M, Puca L, Rosati R, *et al*: Personalized in vitro and in vivo cancer models to guide precision medicine. Cancer Discov 7: 462-477, 2017.